

On the possibilities of merging additive manufacturing and powder injection molding in the production of metal parts

Martin Novák and Berenika Hausnerova

Department of Production Engineering, Faculty of Technology, Tomas Bata University in Zlin, Zlin, Czech Republic and
Centre of Polymer Systems, University Institute, Tomas Bata University in Zlin, Zlin, Czech Republic

Vladimir Pata

Department of Production Engineering, Faculty of Technology, Tomas Bata University in Zlin, Zlin, Czech Republic, and

Daniel Sanetrnik

Centre of Polymer Systems, University Institute, Tomas Bata University in Zlin, Zlin, Czech Republic

Abstract

Purpose – This study aims to enhance merging of additive manufacturing (AM) techniques with powder injection molding (PIM). In this way, the prototypes could be 3D-printed and mass production implemented using PIM. Thus, the surface properties and mechanical performance of parts produced using powder/polymer binder feedstocks [material extrusion (MEX) and PIM] were investigated and compared with powder manufacturing based on direct metal laser sintering (DMLS).

Design/methodology/approach – PIM parts were manufactured from 17-4PH stainless steel PIM-quality powder and powder intended for powder bed fusion compounded with a recently developed environmentally benign binder. Rheological data obtained at the relevant temperatures were used to set up the process parameters of injection molding. The tensile and yield strengths as well as the strain at break were determined for PIM sintered parts and compared to those produced using MEX and DMLS. Surface properties were evaluated through a 3D scanner and analyzed with advanced statistical tools.

Findings – Advanced statistical analyses of the surface properties showed the proximity between the surfaces created via PIM and MEX. The tensile and yield strengths, as well as the strain at break, suggested that DMLS provides sintered samples with the highest strength and ductility; however, PIM parts made from environmentally benign feedstock may successfully compete with this manufacturing route.

Originality/value – This study addresses the issues connected to the merging of two environmentally efficient processing routes. The literature survey included has shown that there is so far no study comparing AM and PIM techniques systematically on the fixed part shape and dimensions using advanced statistical tools to derive the proximity of the investigated processing routes.

Keywords Powder injection molding, Material extrusion, Powder bed fusion, Environmentally benign binder, Advanced statistics, Surface roughness, Strength, Ductility

Paper type Research paper

1. Introduction

The techniques and process parameters of powder injection molding (PIM) and the corresponding additive manufacturing (AM) approaches should result in products of similar quality. However, for both technologies, there are still inherent compromises in the compositions of the materials, product design, process parameters and resulting properties, such as sintered density, residual stresses and mechanical integrity (Bengisu, 2001; Chen *et al.*, 2019; German, 2011; Guo *et al.*, 2017; Hinojos *et al.*, 2016; Nötzel *et al.*, 2018; Wu *et al.*, 2014). The possibility of merging high-volume PIM and individual-to-medium-volume AM opens and broadens innovative

The current issue and full text archive of this journal is available on Emerald Insight at: <https://www.emerald.com/insight/1355-2546.htm>



Rapid Prototyping Journal
30/11 (2024) 50–58
Emerald Publishing Limited [ISSN 1355-2546]
[DOI 10.1108/RPJ-02-2023-0047]

© Martin Novák, Berenika Hausnerova, Vladimir Pata and Daniel Sanetrnik. Published by Emerald Publishing Limited. This article is published under the Creative Commons Attribution (CC BY 4.0) licence. Anyone may reproduce, distribute, translate and create derivative works of this article (for both commercial and non-commercial purposes), subject to full attribution to the original publication and authors. The full terms of this licence may be seen at <http://creativecommons.org/licenses/by/4.0/legalcode>

This work was by the internal grants of [TBU in Zlin] under Grant [No. IGA/FT/2021/006]; and [Ministry of Education, Youth and Sports of the Czech Republic – DKRVO] under Grant [RP/CPS/2022/003].

Ethical compliance: All procedures performed in studies involving human participants were in accordance with the ethical standards of the institutional and/or national research committee and with the 1964 Helsinki Declaration and its later amendments or comparable ethical standards.

Author contributions: Conceptualization: BH; methodology: BH, MN; validation: [MN]; formal analysis: MN and VP; investigation: MN, VP, DS; data curation: MN; writing – original draft preparation: MN; writing – review and editing: BH; visualization: MN; supervision BH; project administration: BH; funding acquisition: BH.

Disclosure statement: The authors have no competing interests relevant to the content of this article to declare.

Received 9 February 2023
Revised 29 September 2023
Accepted 14 January 2024

applications where specific needs benefit from sharing the common features of both processes (Nötzel *et al.*, 2018).

Material extrusion (MEX)-based AM techniques enable efficient production without the need for a mold or tooling (Ebel, 2019; Vyas *et al.*, 2017), thereby balancing the advantages of AM rapid prototyping and PIM high volumes. There is a minimum powder loading, which must be achieved for a part to be sinterable, but at the same time, high-loaded filaments are brittle and impossible to spool (Kukla *et al.*, 2016). The strength limitations of the filaments originate from the viscosity and surface tension of the material, which directly impact the layer-to-layer sintering/bond formation of MEX parts (Fallon *et al.*, 2019; Mackay, 2018; Young *et al.*, 2018, 2019). This is further complicated by the existence of the theoretical maximum viscosities of melts that can be produced with MEX (Fallon *et al.*, 2019) as well as through PIM (Mukund *et al.*, 2015).

Successful examples of developed filaments were reported for copper in acrylonitrile-butadiene-styrene copolymer (Sa'ude *et al.*, 2013), for iron powder in polyamide (Masood and Song, 2004) and for alumina in low density polyethylene/paraffin-based binders (Nötzel *et al.*, 2018). The feasibility of using feedstocks filled with 47 Vol.% of zirconia powder processed by fused deposition modeling (FDM), a type of MEX technique, was investigated (Cano *et al.*, 2019; Gonzalez-Gutierrez *et al.*, 2018). The 55 Vol.% feedstocks for mullite, fused silica and titanium dioxide ceramic powders were prepared (Onagoruwa *et al.*, 2001). The same loading was achieved using a binder system developed by Kukla *et al.* (2016, 2017) for 316L, Ti6Al4V, NdFeB and SrFe powders. Some MEX techniques allow for higher powder loading if a paste is used instead of solid filaments, as proposed by Lu *et al.* (2008) for 60 Vol.% alumina feedstocks.

Typically, it is easier to use the plunger or screw approaches with granules, which are not limited in powder concentration as filaments (Singh *et al.*, 2021). In the case of the screw-based approach, the disadvantage is the maximum extrusion flow rate given by the need for a certain dwell time in a heated printing head dedicated to melting similar to a filament-based approach. Meanwhile, the plunger-based approaches tend to be less precise in the start/stop stages of the printing, and there are also issues connected to the flow control due to feedstock compressibility (Micllette *et al.*, 2022; Côté *et al.*, 2023).

However, there are attempts to develop a filament-based approach to reach sufficient loading percentages, whereas keeping the filament flexible enough to unspool without breaking. In this respect, atomic diffusion AM (ADAM) should be highlighted, as it represents the FDM technique, which uses a standard FDM filament made of metal powders mixed with thermoplastic polymers serving as a binder for highly filled compounds (Galati and Minetola, 2019).

Similarly, feedstocks for PIM have been developed largely on empirical attempts, with limited studies devoted to the quantification of the interactions among particular feedstock components (Bleyan *et al.*, 2015a; Bleyan *et al.*, 2015b; Hausnerova *et al.*, 2016). In this study, a recently developed (Bleyan *et al.*, 2015a; Bleyan, Svoboda, *et al.*, 2015b) environmentally benign binder was used, which allows processing at lower temperatures than commercially available polyolefin-based binders.

The mechanical and surface properties of AM and PIM parts are governed by different process parameters. The surface properties of some AM parts have rarely been compared with those of conventional processing routes. Ruppert *et al.* (2017) obtained a mean surface roughness of $23 \mu\text{m}$ (R_a) via electron beam melting (EBM), whereas direct metal laser sintering (DMLS), which is a type of powder bed fusion technique (PBF), revealed an R_a value of $10 \mu\text{m}$ for titanium implants. Costa Valente *et al.* (2021) compared the surface roughness obtained by another PBF technique, selective laser melting (SLM) and standard machining for Ti6Al4V dental implants and showed that SLM samples had lower wettability and rougher surfaces. Weißmann *et al.* (2018) tested EBM and SLM on Ti6Al4V and reported a significant impact of surface roughness (higher for EBM) on cellular viability. Vaithilingam *et al.* (2016) studied the cytotoxicity of SLM with and without mechanical polishing of Ti6Al4V and found almost no dissolution of metal ions into the cell medium for both surfaces. Padrós *et al.* (2020) compared DMLS with casting (low-wax) and computer aided design/computer aided manufacturing milling of chrome-cobalt alloy dental prosthesis restorations and obtained the highest Vickers hardness and roughest surface for the DMLS samples.

The EBM and DMLS methods were also compared by Soyama and Takeo (2020), who attributed the differences between the roughness of Ti6Al4V alloy manufactured samples to the differences in their mean particle size; R_z was 1.5 times larger than that of the diameter of the used particles for both the DMLS and EBM specimens. It was found (Shunmugavel *et al.*, 2017) that this alloy (Ti6Al4V) processed through SLM provided lower surface roughness after machining than a standard wrought stock; however, it was less ductile and required higher cutting forces. It was also shown (Beaucamp *et al.*, 2015) that the unacceptable surface of Ti6Al4V manufactured with EBM and SLS samples can be smoothed to less than 10 nm (R_a) with shape-adaptive grinding.

Surface roughness also affects the oxidation rate of samples during their lifespan, as pointed out by Sanviemvongsak *et al.* (2018) for the IN718 alloy, where as-built EBM samples with raw surfaces show higher oxidation kinetics than SLM samples and the wrought alloy because of their higher surface area. Metallographic, crystallographic and topographic analyses of DMLS, EBM and wrought Ti6Al4V samples (Acquesta and Monetta, 2020) carried out on as-produced AM specimens, together with potentiodynamic polarization tests, revealed significantly different microstructures and electrochemical behaviors when compared to the traditionally produced specimen; however, the differences substantially diminished after mechanical polishing.

Our research aims to compare the mechanical properties of sintered 17-4PH steel items with respect to surfaces created through DMLS, MEX (specifically ADAM technique) and PIM of the recently developed feedstock based on polyethylene glycol and acrawax binders. Selection of the AM methods follows the intention to demonstrate the similarities/differences between AM (MEX) similar to PIM and AM (DMLS) different from PIM, highlighting the presence of the unique processing features on the surfaces. In addition, DMLS powders were also used for the preparation of samples with PIM to intercept the influence of particle size and size

distribution of powder on the rheological, final mechanical and surface properties of PIM.

2. Materials and methods

Stainless steel 17-4PH (Sandvik Osprey Ltd., $D_{50} = 31.8 \mu\text{m}$) was used to produce DMLS samples on an EOS M290 (EOS GmbH, Germany) using 400 W Yb-fiber laser. The layer thickness was 0.05 mm, maximum build dimensions were $250 \times 250 \times 325 \text{ mm}$. Samples were sintered in a flat position. The samples designated as DMLS_{Blasted} were treated with sandblasting. MEX samples were manufactured using a Metal X system (Markforged, the USA) with Markforged WASH-1 as a debinding system. The infill was 100% using a $+45^\circ/-45^\circ$ infill angle. The layer thickness was 0.15 mm, and the nozzle diameter was 0.4 mm.

PIM samples (designated PIM_{PIM}) were prepared from the feedstock containing stainless steel 17-4PH PIM-grade powder (Sandvik Osprey Ltd., $D_{50} = 8.2 \mu\text{m}$). Additionally, 17-4PH steel powder ($D_{50} = 31.8 \mu\text{m}$) used for DMLS samples was also used to prepare PIM feedstocks (abbreviated PIM_{DMLS}) to compare the effect of particle size and size distribution on this manufacturing approach. Particle size distributions were evaluated with a laser diffraction particle size analyzer (Malvern Mastersizer 3000, Malvern Panalytical Ltd, Malvern, the UK), as shown in Figure 1.

A recently developed binder (Hausnerova and Novak, 2020) containing PEG4000/PEG6000/AW/PW/SA (29.5/29.5/28/12/1) Wt.% was selected to compound 60 Vol.% feedstocks on a counter-rotating twin-screw extruder (Plasti-corder PL 2000, Brabender GmbH & Co, Duisburg, Germany). Two-round extrusion was performed with temperature profiles of 90/75/70°C and 65/60/55°C for PIM_{DMLS} and PIM_{PIM}, respectively.

The rheological properties of the feedstocks relevant for PIM as well as MEX were determined using a capillary rheometer (Göettfert 50, GÖTTFERT Werkstoff-Prüfmaschinen GmbH, Buchen, Germany) with a capillary length-to-diameter (L/D) ratio of 20/0.5 and 20/1 at the apparent shear rate range of $35\text{--}4,000 \text{ s}^{-1}$

and corresponding processing temperatures. Rheological measurements (Figure 2) illustrate the complex dilatant and pseudoplastic behavior of the PIM feedstocks. The optimum feedstock viscosity for injection molding has been empirically determined to be up to $10^3 \text{ Pa}\cdot\text{s}$ at shear rates between 10^2 and 10^5 s^{-1} (Dihoru *et al.*, 2000). Therefore, the PIM_{DMLS} feedstock showed viscosity at the upper limit of the optimal value for a certain range of shear rates. The changes in flow from a pseudoplastic to a dilatant indicate that particles could not form layers and slide over each other as shown, e.g. by Hausnerova (2011). During rheological tests on a 20/0.5 capillary, a binder separation accompanied by an accumulation of powder particles on the walls was observed for the PIM_{DMLS} feedstock. A larger capillary diameter (20/1) was also tested, but the significant pressure instabilities at higher shear rates led to exclusion of the obtained values. For the MEX filament, a significant degradation of the material was observed during testing at 220°C (the temperature recommended by the filament supplier). However, a relatively low viscosity with a favorable pseudoplastic cause was obtained when the temperature was lowered to 200°C.

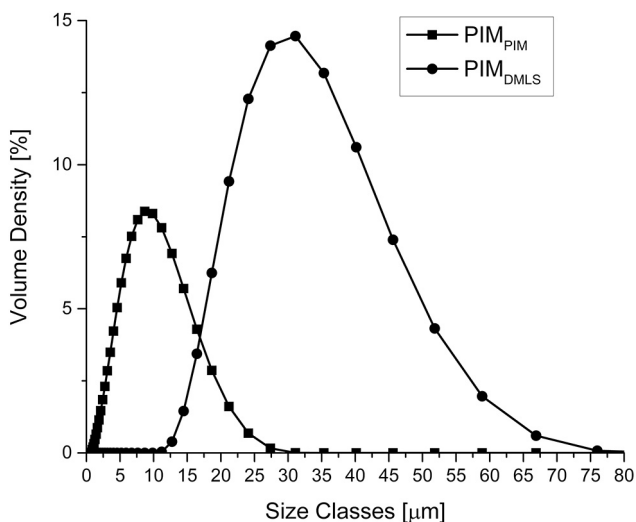
Following injection molding was performed on a PIM machine (Allrounder 370S, Arburg, ARBURG GmbH + Co KG, Lössburg, Germany). The molding conditions are listed in Table 1, the testing specimens were type A according to EN ISO 2740:2009(E).

Thermal debinding and sintering of PIM_{DMLS}, PIM_{PIM} and MEX were performed in a sintering furnace (CLASIC CZ s r. o., Revnice, Czech Republic) under the conditions, as shown in Table 2 and Figure 3. Micrographs of compounds were obtained using a scanning electron microscope (SEM; VEGA II LMU, Tescan Ltd., Czech Republic). An operating voltage of 30 kV was used.

The density after sintering was obtained using the Archimedes method on the samples (five for each series) made from a grip section of the bars for the tensile tests. MEX, PIM_{PIM}, PIM_{DMLS}, DMLS and DMLS_{Blasted} revealed values of 7.33 ± 0.20 , 7.23 ± 0.04 , 7.11 ± 0.05 , 7.83 ± 0.02 and $7.85 \pm 0.02 \text{ g/cm}^3$, respectively. The values of DMLS and DMLS_{Blasted} are higher than 7.8 g/cm^3 of standardly machined 17-4PH steel according to the data sheet [1], which is in accordance with Gu *et al.* (2013). Relative densities of samples are then 94.0, 92.7, 91.1, 100.4 and 100.6% for MEX, PIM_{PIM}, PIM_{DMLS}, DMLS and DMLS_{Blasted}, respectively, of the traditionally made 17-4 PH steel. The powder loading of the MEX samples was calculated under the assumption that $V_{Sint} = V_S/d_r$, where V_{Sint} and V_S represent the volumes of the sintered sample and the fully dense 17-4PH steel, respectively, and d_r is the relative density of the sintered sample. The full volume of the sample was derived from the enlargement rate (opposite to the shrinkage rate). The green samples from the MEX feedstock were approximately 1.16 times larger than the sintered samples in a linear direction, which resulted in the volume of the green sample V_0 being 1.56 times larger than V_{Sint} , which is 1.06 times larger than V_S . Then, the calculated powder loading was 60.5 Vol.%.

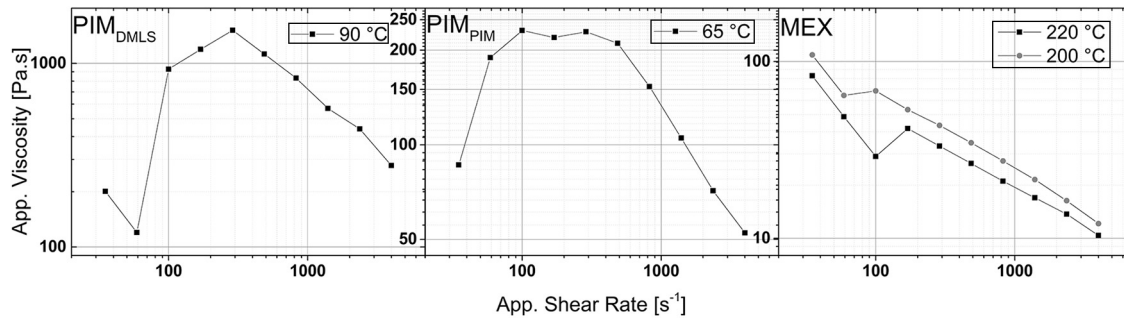
The strain at break, tensile strength and yield strength (YS) were evaluated using a tensile testing machine (ZWICK Materialprüfung, 1456, ZwickRoell GmbH & Co.KG, Ulm, Germany) according to the ASTM standard method E8M-00. The gauge length was 40 mm, crosshead speed was 0.7 mm/min. Strain at break was taken as a maximum elongation detected

Figure 1 Particle size distributions of PIM and DMLS powders



Source: Figure by authors

Figure 2 Apparent viscosity as a function of apparent shear rate of feedstocks intended for injection molding based on PIM and DMLS powders and filaments processed via MEX



Source: Figure by authors

Table 1 Optimized injection molding parameters

Parameter	Value
Temperature – nozzle (°C)	75
Temperature – zone 1 (°C)	95
Temperature – zone 2 (°C)	85
Temperature – zone 3 (°C)	80
Temperature – zone 4 (°C)	75
Temperature – zone 5 (°C)	20
Screw stroke (mm)	60
Cooling time (s)	30
Injection pressure (bar)	1,000
Hold pressure/time 1 (bar/s)	800/5
Hold pressure/time 2 (bar/s)	150/2

Source: Table by authors

Table 2 Mechanical properties of DMLS, ADAM and PIM samples

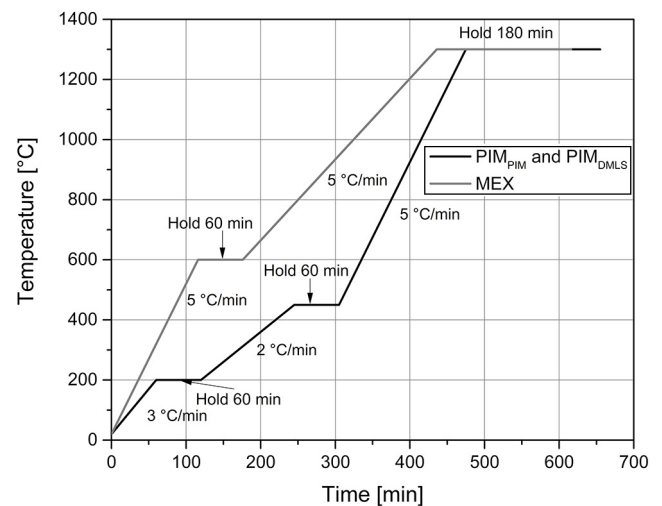
Method	Ultimate tensile		Strain at break (%)
	strength (MPa)	Yield strength (MPa)	
PIM _{DMLS}	750 ± 47	640 ± 56	2.1 ± 0.3
PIM _{PIM}	980 ± 14	800 ± 14	3.3 ± 1.6
DMLS	1140 ± 15	510 ± 17	19 ± 0.9
DMLS _{blasted}	1140 ± 6.7	510 ± 11	18 ± 2.2
ADAM	880 ± 8.0	730 ± 11	4.5 ± 0.3

Source: Table by authors

during measurement at the point of breaking including both elastic and plastic parts of the strain. Five samples were measured for each of the series.

A 3D scanner (TALYSURF CLI 500, Taylor Hobson, Leicester, the UK) was used for surface scanning. Standard surface roughness parameters, including the arithmetic mean deviation from the centerline of the profile (*Ra*), profile maximum height (*Rz*) and profile average distance of microscopic unevenness (*RSm*) were measured. As these characteristic parameters are tied with both random and systematic errors, they were carefully treated with the principal components method and cluster analysis to increase the reliability of the data obtained. The sampling rate was 20 Hz in the maximum interface measurement mode. The measured

Figure 3 Sintering profiles for MEX and PIM samples



Source: Figure by authors

area was 4 × 4 mm (according to ISO, 4288) with 25 μm spacing, providing a resolution of 161 traces for each measurement.

The data were treated with advanced statistical tools – method of principal components (PCA) and cluster analysis (CA) – Ward method. CA in general serves to categorize units into groups (clusters) based on their similarity. Ward method specifically is a type of variance method, which generates clusters via minimization of a cluster heterogeneity (and not based on an optimization of distances between them). It uses the sum-of-squares criterion to produce the groups, which minimize the dispersion within a group at each binary fusion, and therefore, it tends to create relatively small clusters (Murtagh and Legendre, 2014).

PCA is a multivariate statistical method that combines information from several variables observed on the same subjects into fewer variables. These variables are then called PCA. They can have a positive or negative influence indicated by a plus or minus sign. The first component describes the largest part of the variance of original data, the second component describes the largest part of variance not included in the first component and so on, with the maximum number of

components equal to the number of the variables investigated. The first two components can be transformed into scatterplots, which allow for an intuitive interpretation of the main features present in the complex multivariate data set through the graphical display (Greenacre et al., 2022).

The combination of these two methods allows to quantify the similarity and intercept surfaces with similar parameters with a particular probability.

3. Results and discussion

The mechanical properties of the samples produced using the investigated processing routes are summarized in Table 2. The ultimate tensile strength (UTS) and ductility (strain at break) of the DMLS samples were the highest. PIM samples based on PIM-quality (PIM_{PIM}) powders resulted in the second-highest UTS and the highest YS, regardless of blistering occurring after sintering on flat parts of the testing samples. The shrinkage of PIM_{PIM} samples was approximately 14%, which agreed with the reported approximately 15% value for martensitic stainless steels (Blaine et al., 2003). Blistering on certain places of the PIM_{PIM} samples persisted even with the longer debinding time allowed in a water bath (10 h instead of 7 h) and with the use of a nitrogen atmosphere during thermal debinding.

This was likely not an issue for PIM_{DMLS} samples because of the larger size of the particles, which can be debound faster (Sotomayor et al., 2010). However, the PIM_{DMLS} samples in a nitrogen atmosphere exhibited a high degree of nitridation and shrunk only by approximately 8% of their original size. After the change to the hydrogen atmosphere, the shrinkage increased up to 12%, indicating still unacceptably high porosity, which caused the lower mechanical properties (Table 2). Therefore, a hydrogen atmosphere was used in all experiments.

Overall, the UTS of all samples except for PIM_{DMLS} exceeded the value reported in the literature (German, 2018) (UTS of 820 MPa before heat treatment). Both the MEX and PIM_{PIM} parts had significantly higher YS than those created by the DMLS technique. It should be mentioned that the performance of the sintered parts can be substantially improved with heat treatment as shown, e.g. by Pellegrini et al. (2023).

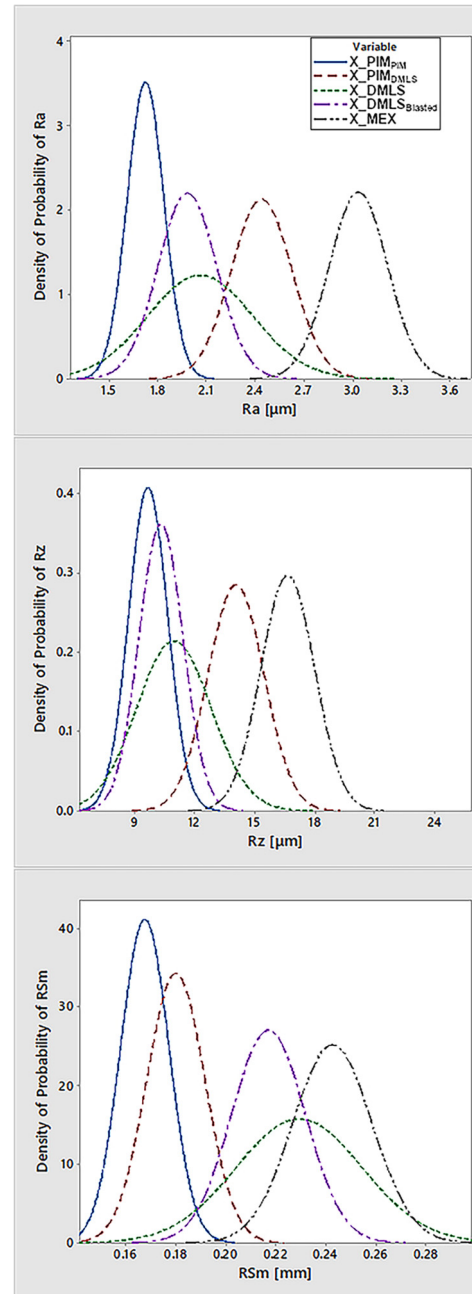
As can be seen in Table 3 and Figure 4, PIM_{PIM} has the smoothest surface. The typical drawbacks of PIM compounds as powder/binder separation (Sanetnik et al., 2018, 2019) were not observed in the samples after injection molding. Its mean *RSm* value of 16.75 μm indicates that the surface reproduces the size of the individual particles (90% of which had a size of 16 μm and less).

Table 3 Surface parameters (mean values) of DMLS, ADAM and PIM samples

Method	<i>Ra</i> (μm)	<i>Rz</i> (μm)	<i>RSm</i> (μm)	<i>Rz/RSm</i>
PIM _{DMLS}	2.44 ± 0.19	14.08 ± 1.40	17.99 ± 1.16	0.78
PIM _{PIM}	1.73 ± 0.11	9.68 ± 0.98	16.75 ± 0.97	0.58
DMLS	2.06 ± 0.32	10.97 ± 1.86	22.93 ± 2.53	0.48
DMLS _{Blasted}	1.98 ± 0.18	10.32 ± 1.10	21.70 ± 1.47	0.48
ADAM	3.04 ± 0.18	16.67 ± 1.34	24.26 ± 1.58	0.69

Source: Table by authors

Figure 4 Histograms of *Ra*, *Rz* and *RSm* surface parameters for tested samples



Source: Figure by authors

Sandblasting of DMLS reduced the standard deviation of the *Ra* parameter from 0.32 μm to 0.18 μm.

The *RSm* parameter shows the frequency of the amplitudes, that is, how often the dip in the surface is detected. Both PIM samples exhibited lower *RSm* values, indicating a higher frequency of dips. This shows the dependence of the surface quality of the PIM-created samples on the size and type of powder. It also likely indicates a greater degree of fusing when the same powder is used in DMLS, as DMLS and DMLS_{Blasted} samples have greater *RSm* values than PIM_{DMLS}. This is

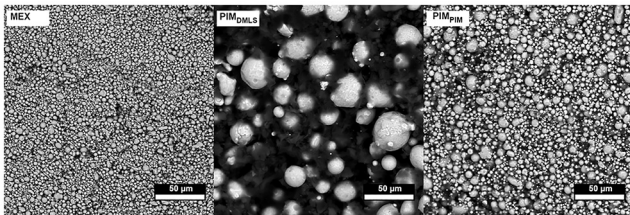
supported by an Ra of $1.73\ \mu\text{m}$ for PIM_{PIM} . The surface parameters of MEX were similar to those obtained recently by Lavecchia *et al.* (2023), where Ra in a direction parallel to the deposition of the filament reaches $1.5\ \mu\text{m}$, and $4.7\ \mu\text{m}$ if scanned orthogonally to the deposition.

It is assumed that for debinding- and sintering-based methods such as PIM and MEX, the surface roughness is governed by the size of the particles as they are not fused to the same degree as during laser sintering, resulting in substantially higher ductility of the DMLS samples. The gradual densification and resulting changes in microstructure are well documented in the literature, e.g. in Blaine *et al.* (2003). Thus, higher surface porosity can be expected for both PIM and MEX sintered samples. Thus, the surface scanner would then be less likely to detect dips for DMLS samples, as reflected by the higher Rz/RSm ratio, showing a possible correlation between this ratio and ductility.

The development of sintering bonds can be estimated using a sintering model (Pokluda *et al.*, 1997), which shows the importance of the initial particle size and sintering time without considering the effect of the mold surface itself. The sizes of the particles used can be revealed from the SEM images of the feedstocks, as shown in Figure 5. Based on this model, the time required for sintering larger particles was longer.

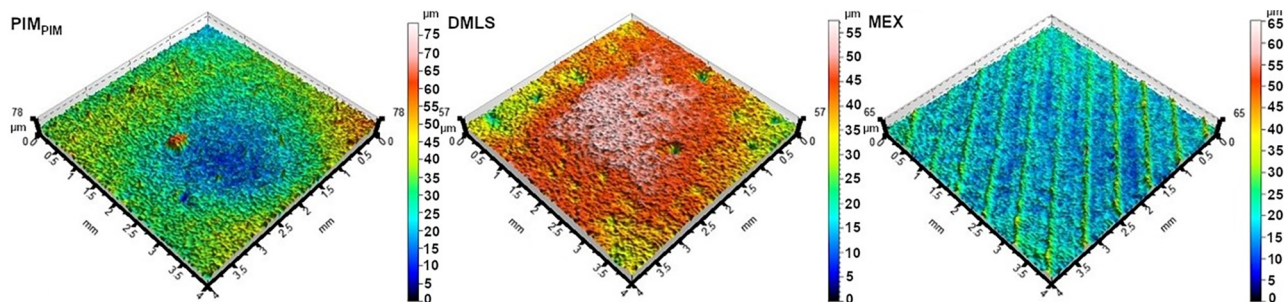
However, in this study, the sintering time (final dwell time) was kept the same, and therefore, the degree of fusion between larger powder particles should be lower. In this case, RSm should increase, whereas both Ra and Rz decrease. In particular, Rz/RSm ratio should approach 1 if the particles are not properly fused. This applies to finer PIM_{PIM} particles

Figure 5 SEM of MEX, PIM_{DMLS} and PIM_{PIM} feedstocks (BSE mode at $1,000\times$ magnification)



Source: Figure by authors

Figure 6 3D surface maps of PIM_{PIM} , DMLS and MEX sintered parts



Source: Figure by authors

compared to coarser PIM_{DMLS} but does not explain the cause of the MEX samples.

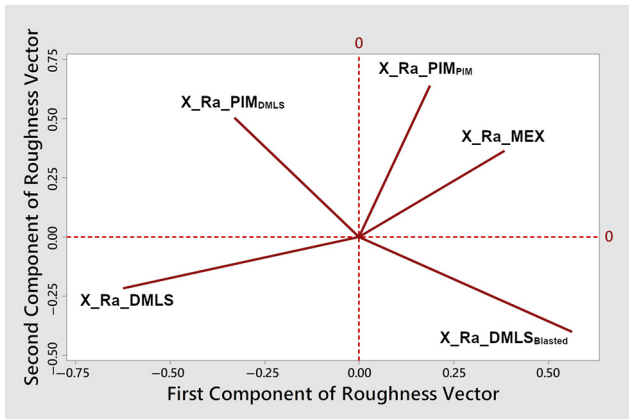
Generally, the differences in the surface properties are attributed not only to the particle size of the powders but also to the feedstock compositions and process parameters used (Hausnerova *et al.*, 2018). The powder loading in the MEX samples, which is one of the most relevant factors, is similar to the loading used in PIM feedstocks; therefore, it is assumed that this is not the case here. The relative density of the sintered samples was also higher for MEX than for PIM. Therefore, this discrepancy may be attributed to the processing methods used. The 3D maps of the surfaces of the PIM_{PIM} , DMLS and MEX samples are shown in Figure 6, depicting the differences in the surface structure provided by each method. PIM_{PIM} samples have individual peaks, DMLS parts show typical significant pits on the surface and MEX results in noticeable tracks, which are remnants of the interface between the particular filament layers. Presented 3D surface maps intercept both the roughness and the waviness of the surface parts. However, with fast Fourier transformation applied, the waviness part is removed, and thus the possibility of distortion of the numerical values of the Ra parameter resulting from the surface waviness is eliminated.

To quantify the surface similarities created through different manufacturing routes, the Ra parameter was further statistically analyzed using the PCA and CA Ward method. The loading plot obtained through the test A method (Figure 7) suggests the similarity between PIM_{DMLS} and DMLS, which have negative first components, and among PIM_{PIM} , MEX and $\text{DMLS}_{\text{Blasted}}$ deviating from these two.

The similarity level (Figure 8) between PIM_{PIM} and MEX was approximately 58% according to CA, and between DMLS and PIM_{DMLS} it reached 53%, whereas $\text{DMLS}_{\text{Blasted}}$ was similar to PIM_{PIM} and MEX at approximately 45%. The similarity between the two cluster groups (PIM_{PIM} , MEX and $\text{DMLS}_{\text{Blasted}}$ versus PIM_{DMLS} and DMLS) was only 32%.

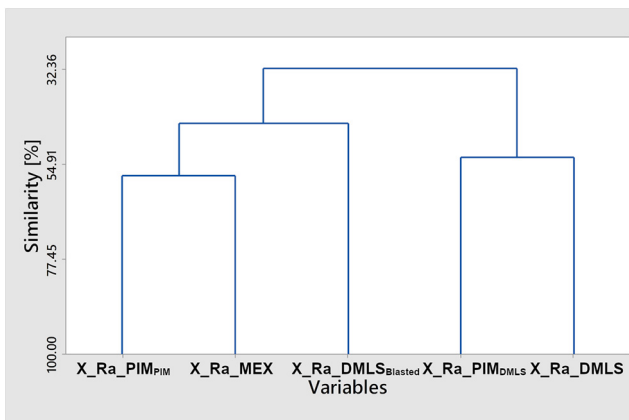
Overall, a degree of similarity of less than 60% is rather low. As expected, the $\text{DMLS}_{\text{Blasted}}$ samples appeared to be unique in all statistical examinations. Nevertheless, through this investigation, together with observations from histograms and box plots (Figure 9), PIM_{PIM} provided the smoothest surface to the final sintered samples.

Figure 7 Loading plot for PIM_{PIM}, PIM_{DMLS}, DMLS, DMLS_{Blasted} and MEX obtained through the principal component statistical method



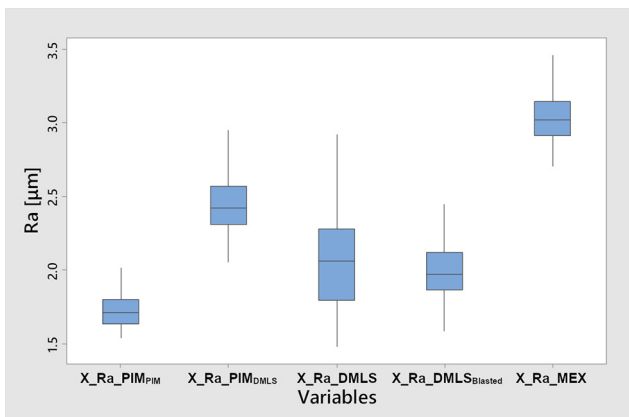
Source: Figure by authors

Figure 8 Dendrogram for PIM_{PIM}, PIM_{DMLS}, DMLS, DMLS_{Blasted} and MEX obtained through Ward cluster method



Source: Figure by authors

Figure 9 Boxplots of Ra surface parameter for PIM_{PIM}, PIM_{DMLS}, DMLS, DMLS_{Blasted} and MEX samples



Source: Figure by authors

4. Conclusion

The surface properties and mechanical performance of powder manufacturing techniques based on sintering (DMLS), debinding and sintering (PIM and MEX) were investigated in this study. During DMLS, the powder fully melts and fuses layer by layer, whereas, during PIM and MEX, they are sintered slightly below the melting temperatures. The surfaces of the samples created using PIM technology were smooth without the necessity of finishing operations. Statistical analysis based on the principal component method and cluster analysis showed close to 60% similarity between surfaces created via PIM_{PIM} and MEX. The sintered parts produced using MEX and PIM_{PIM} also had similar relative densities. However, the MEX samples showed the worst absolute values for the Ra and Rz surface parameters. The samples created with the DMLS powders were rather different, regardless of the method used. Finally, PIM parts made from eco-friendly PEG and AW-based feedstock may successfully compete with the DMLS samples, which showed the highest mechanical strength.

Note

- 1 www.upmet.com/sites/default/files/datasheets/17-4-ph.pdf

References

- Acquesta, A. and Monetta, T. (2020), “As-built EBM and DMLS Ti-6Al-4V parts: topography–corrosion resistance relationship in a simulated body fluid”, *Metals*, Vol. 10 No. 8, p. 1015, doi: [10.3390/met10081015](https://doi.org/10.3390/met10081015).
- Beaucamp, A.T., Namba, Y., Charlton, P., Jain, S. and Graziano, A.A. (2015), “Finishing of additively manufactured titanium alloy by shape adaptive grinding (SAG)”, *Surface Topography: Metrology and Properties*, Vol. 3 No. 2, p. 24001, doi: [10.1088/2051-672X/3/2/024001](https://doi.org/10.1088/2051-672X/3/2/024001).
- Bengisu, M. (2001), *Engineering Ceramics*, Springer Science & Business Media, Berlin.
- Blaine, D., Wu, Y., Schlaefler, C. and Marx, B. (2003), “Sintering shrinkage and microstructure evolution during densification of a martensitic stainless steel”, paper presented at the Sintering Conference, 4 September, PA State University, PA, available at: www.researchgate.net/publication/237282609 (accessed 7 February 2023).
- Bleyan, D., Hausnerova, B. and Svoboda, P. (2015a), “The development of powder injection moulding binders: a quantification of individual components’ interactions”, *Powder Technology*, Vol. 286, pp. 84–89, doi: [10.1016/j.powtec.2015.07.046](https://doi.org/10.1016/j.powtec.2015.07.046).
- Bleyan, D., Svoboda, P. and Hausnerova, B. (2015b), “Specific interactions of low molecular weight analogues of carnauba wax and polyethylene glycol binders of ceramic injection moulding feedstocks”, *Ceramics International*, Vol. 41 No. 3, pp. 3975–3982, doi: [10.1016/j.ceramint.2014.11.082](https://doi.org/10.1016/j.ceramint.2014.11.082).
- Cano, S., Gonzalez-Gutierrez, J., Sapkota, J., Spoerk, M., Arbeiter, F., Schuschnigg, S., Holzer, C. and Kukla, C. (2019), “Additive manufacturing of zirconia parts by fused filament fabrication and solvent debinding: selection of binder formulation”, *Additive Manufacturing*, Vol. 26, pp. 117–128, doi: [10.1016/j.addma.2019.01.001](https://doi.org/10.1016/j.addma.2019.01.001).

- Chen, Z., Li, Z., Li, J., Liu, C., Lao, C., Fu, Y., Liu, C., Li, Y., Wang, P. and He, Y. (2019), “3D printing of ceramics: a review”, *Journal of the European Ceramic Society*, Vol. 39 No. 4, pp. 661–687, doi: [10.1016/j.jeurceramsoc.2018.11.013](https://doi.org/10.1016/j.jeurceramsoc.2018.11.013).
- Costa Valente, M.L., Oliveira, T.T., Kreve, S., Batalha, R.L., Oliveira, D.P., Pauly, S., Bolfarini, C., Bachmann, L. and Dos Reis, A.C. (2021), “Analysis of the mechanical and physicochemical properties of Ti-6Al-4 V discs obtained by selective laser melting and subtractive manufacturing method”, *Journal of Biomedical Materials Research Part B: Applied Biomaterials*, Vol. 109 No. 3, pp. 420–427, doi: [10.1002/jbm.b.34710](https://doi.org/10.1002/jbm.b.34710).
- Côté, R., Demers, V., Demarquette, N.R., Charlon, S. and Soulestin, J. (2023), “A strategy to eliminate interbead defects and improve dimensional accuracy in material extrusion 3D printing of highly filled polymer”, *Additive Manufacturing*, Vol. 68, p. 103509, doi: [10.1016/j.addma.2023.103509](https://doi.org/10.1016/j.addma.2023.103509).
- Dihoru, L.V., Smith, L.N., Orban, R. and German, R.M. (2000), “Experimental study and neural network modeling of the stability of powder injection molding feedstocks”, *Materials and Manufacturing Processes*, Taylor & Francis, Vol. 15 No. 3, pp. 419–438, doi: [10.1080/10426910008912997](https://doi.org/10.1080/10426910008912997).
- Ebel, T. (2019), “PMTi2019: international conference on the PM and AM of titanium highlights a bright future for sinter-based technologies”, *Powder Injection Moulding International*, Vol. 13 No. 4, pp. 61–74.
- Fallon, J.J., McKnight, S.H. and Bortner, M.J. (2019), “Highly loaded fiber filled polymers for material extrusion: a review of current understanding”, *Additive Manufacturing*, Vol. 30, p. 100810, doi: [10.1016/j.addma.2019.100810](https://doi.org/10.1016/j.addma.2019.100810).
- Galati, M. and Minetola, P. (2019), “Analysis of density, roughness, and accuracy of the atomic diffusion additive manufacturing (ADAM) process for metal parts”, *Materials*, Vol. 12 No. 24, doi: [10.3390/ma12244122](https://doi.org/10.3390/ma12244122).
- German, R.M. (2011), *Metal Injection Molding: A Comprehensive MIM Design Guide*, Metal Powder Industries Federation, Princeton, NJ.
- German, R.M. (2018), “17-4 PH stainless steel: a guide to debinding and sintering for MIM-like AM processes published”, *Powder Injection Moulding International*, Vol. 12 No. 2, pp. 49–75.
- Gonzalez-Gutierrez, J., Cano, S., Schuschnigg, S., Kukla, C., Sapkota, J. and Holzer, C. (2018), “Additive manufacturing of metallic and ceramic components by the material extrusion of highly-filled polymers: a review and future perspectives”, *Materials*, Vol. 11 No. 5, p. 840, doi: [10.3390/ma11050840](https://doi.org/10.3390/ma11050840).
- Greenacre, M., Groenen, P.J.F., Hastie, T., D’Enza, A.I., Markos, A. and Tuzhilina, E. (2022), “Principal component analysis”, *Nature Reviews Methods Primers*, Vol. 2 No. 1, doi: [10.1038/s43586-022-00184-w](https://doi.org/10.1038/s43586-022-00184-w).
- Gu, H., Gong, H., Pal, D., Rafi, K., Starr, T.L. and Stucker, B.E. (2013), “Influences of energy density on porosity and microstructure of selective laser melted 17-4PH stainless steel”, in Bourell, D.L. (Eds), *24th Annual International Solid Freeform Fabrication Symposium: An Additive Manufacturing Conference, Proceedings*, The University of TX at Austin, Austin, pp. 474–489, doi: [10.26153/tsw/15572](https://doi.org/10.26153/tsw/15572).
- Guo, P., Zou, B., Huang, C. and Gao, H. (2017), “Study on microstructure, mechanical properties and machinability of efficiently additive manufactured AISI 316L stainless steel by high-power direct laser deposition”, *Journal of Materials Processing Technology*, Vol. 240, pp. 12–22, doi: [10.1016/j.jmatprotec.2016.09.005](https://doi.org/10.1016/j.jmatprotec.2016.09.005).
- Hausnerova, B. (2011), *Rheological Approaches to Powder Injection Moulding Optimization, Qualifying Lecture for Professorship*, Tomas Bata University in Zlín, Zlín.
- Hausnerova, B. and Novak, M. (2020), “Environmentally efficient 316L stainless steel feedstocks for powder injection molding”, *Polymers*, Vol. 12 No. 6, doi: [10.3390/polym12061296](https://doi.org/10.3390/polym12061296).
- Hausnerova, B., Bleyan, D., Kasparkova, V. and Pata, V. (2016), “Surface adhesion between ceramic injection molding feedstocks and processing tools”, *Ceramics International*, Vol. 42 No. 1, pp. 460–465, doi: [10.1016/j.ceramint.2015.08.132](https://doi.org/10.1016/j.ceramint.2015.08.132).
- Hausnerova, B., Sanetnik, D. and Pata, V. (2018), “Surface properties of powder injection moulded parts related to processing conditions”, *Manufacturing Technology*, Vol. 18 No. 6, pp. 895–899, doi: [10.21062/ujep/197.2018/a/1213-2489/mt/18/6/895](https://doi.org/10.21062/ujep/197.2018/a/1213-2489/mt/18/6/895).
- Hinojos, A., Mireles, J., Reichardt, A., Frigola, P., Hosemann, P., Murr, L.E. and Wicker, R.B. (2016), “Joining of inconel 718 and 316 stainless steel using electron beam melting additive manufacturing technology”, *Materials & Design*, Vol. 94, pp. 17–27, doi: [10.1016/j.matdes.2016.01.041](https://doi.org/10.1016/j.matdes.2016.01.041).
- Kukla, C., Duretek, I., Schuschnigg, S., Gonzalez-Gutierrez, J. and Holzer, C. (2016), “Properties for PIM feedstocks used in fused filament fabrication”, in Petzoldt, F. (Ed.), *World PM2016 Congress and Exhibition*, European Powder Metallurgy Association, Shrewsbury, pp. 1–5.
- Kukla, C., Gonzalez-Gutierrez, J., Cano, S., Hampel, S., Burkhardt, C., Moritz, T. and Holzer, C. (2017), “Fused filament fabrication (FFF) of PIM feedstocks”, in Herranz, G., Ferrari, B. and Cabrera, J.M. (Eds), *Actas Del VI Congreso Nacional de Pulvimetalurgia y I Congreso Iberoamericano de Pulvimetalurgia*, Ciudad Real.
- Lavecchia, F., Pellegrini, A. and Galantucci, L.M. (2023), “Comparative study on the properties of 17-4 PH stainless steel parts made by metal fused filament fabrication process and atomic diffusion additive manufacturing”, *Rapid Prototyping Journal*, Vol. 29 No. 2, pp. 393–407, doi: [10.1108/RPJ-12-2021-0350](https://doi.org/10.1108/RPJ-12-2021-0350).
- Lu, X., Lee, Y., Yang, S., Hao, Y., Ubc, R., Evans, J.R.G. and Parini, C.G. (2008), “Fabrication of electromagnetic crystals by extrusion freeforming”, *Metamaterials*, Vol. 2 No. 1, pp. 36–44, doi: [10.1016/J.METMAT.2007.12.001](https://doi.org/10.1016/J.METMAT.2007.12.001).
- Mackay, M.E. (2018), “The importance of rheological behavior in the additive manufacturing technique material extrusion”, *Journal of Rheology*, Vol. 62 No. 6, pp. 1549–1561, doi: [10.1122/1.5037687](https://doi.org/10.1122/1.5037687).
- Masood, S.H. and Song, W.Q. (2004), “Development of new metal/polymer materials for rapid tooling using fused deposition modelling”, *Materials & Design*, Vol. 25 No. 7, pp. 587–594, doi: [10.1016/j.matdes.2004.02.009](https://doi.org/10.1016/j.matdes.2004.02.009).
- Miclette, O., Cote, R., Demers, V. and Brailovski, V. (2022), “Material extrusion additive manufacturing of low-viscosity metallic feedstocks: performances of the plunger-based approach”, *Additive Manufacturing*, Vol. 60, p. 103252, doi: [10.1016/j.addma.2022.103252](https://doi.org/10.1016/j.addma.2022.103252).
- Mukund, B.N., Hausnerova, B. and Shivashankar, T.S. (2015), “Development of 17-4PH stainless steel bimodal powder injection molding feedstock with the help of interparticle

- spacing/lubricating liquid concept”, *Powder Technology*, Vol. 283, pp. 24-31, doi: [10.1016/j.powtec.2015.05.013](https://doi.org/10.1016/j.powtec.2015.05.013).
- Murtagh, F. and Legendre, P. (2014), “Ward’s hierarchical agglomerative clustering method: which algorithms implement ward’s criterion?”, *Journal of Classification*, Vol. 31 No. 3, pp. 274-295, doi: [10.1007/s00357-014-9161-z](https://doi.org/10.1007/s00357-014-9161-z).
- Nötzel, D., Eickhoff, R. and Hanemann, T. (2018), “Fused filament fabrication of small ceramic components”, *Materials*, Vol. 11 No. 8, p. 1463, doi: [10.3390/ma11081463](https://doi.org/10.3390/ma11081463).
- Onagoruwa, S., Bose, S. and Bandyopadhyay, A. (2001), “Fused deposition of ceramics (FDC) and composites”, *Proceedings of the 2001 International Solid Freeform Fabrication Symposium*, The University of TX at Austin, Austin, pp. 224-231, doi: [10.26153/tsw/3267](https://doi.org/10.26153/tsw/3267).
- Padrós, R., Punset, M., Molmeneu, M., Velasco, A.B., Herrero-Climent, M., Rupérez, E. and Gil, F.J. (2020), “Mechanical properties of CoCr dental-prosthesis restorations made by three manufacturing processes. Influence of the microstructure and topography”, *Metals*, Vol. 10 No. 6, p. 788, doi: [10.3390/met10060788](https://doi.org/10.3390/met10060788).
- Pellegrini, A., Lavecchia, F., Guerra, M.G. and Galantucci, L. M. (2023), “Influence of aging treatments on 17–4 PH stainless steel parts realized using material extrusion additive manufacturing technologies”, *The International Journal of Advanced Manufacturing Technology*, Vol. 126 No. 1-2, pp. 163-178, doi: [10.1007/s00170-023-11136-3](https://doi.org/10.1007/s00170-023-11136-3).
- Pokluda, O., Bellehumeur, C.T. and Vlachopoulos, J. (1997), “Modification of Frenkel’s model for sintering”, *AIChE Journal*, Vol. 43 No. 12, pp. 3253-3256, doi: [10.1002/aic.690431213](https://doi.org/10.1002/aic.690431213).
- Ruppert, D.S., Harrysson, O.L.A., Marcellin-Little, D.J., Abumoussa, S., Dahners, L.E. and Weinhold, P.S. (2017), “Osseointegration of coarse and fine textured implants manufactured by electron beam melting and direct metal laser sintering”, *3D Printing and Additive Manufacturing*, Vol. 4 No. 2, pp. 91-97, doi: [10.1089/3dp.2017.0008](https://doi.org/10.1089/3dp.2017.0008).
- Sa’ude, N., Masood, S.H., Nikzad, M., Ibrahim, M. and Ibrahim, M.H.I. (2013), “Dynamic mechanical properties of copper-ABS composites for FDM feedstock”, *International Journal of Engineering Research and Applications*, Vol. 3 No. 3, pp. 1257-1263.
- Sanetnik, D., Hausnerova, B. and Pata, V. (2019), “Online rheometry investigation of flow/slip behavior of powder injection molding feedstocks”, *Polymers*, Vol. 11 No. 3, p. 432, doi: [10.3390/polym11030432](https://doi.org/10.3390/polym11030432).
- Sanetnik, D., Hausnerova, B., Filip, P. and Hnatkova, E. (2018), “Influence of capillary die geometry on wall slip of highly filled powder injection molding compounds”, *Powder Technology*, Vol. 325, pp. 615-619, doi: [10.1016/j.powtec.2017.11.041](https://doi.org/10.1016/j.powtec.2017.11.041).
- Sanviemvongsak, T., Monceau, D. and Macquaire, B. (2018), “High temperature oxidation of in 718 manufactured by laser beam melting and electron beam melting: effect of surface topography”, *Corrosion Science*, Vol. 141, pp. 127-145, doi: [10.1016/j.corsci.2018.07.005](https://doi.org/10.1016/j.corsci.2018.07.005).
- Shunmugavel, M., Polishetty, A., Goldberg, M., Singh, R. and Littlefair, G. (2017), “A comparative study of mechanical properties and machinability of wrought and additive

- manufactured (selective laser melting) titanium alloy – Ti-6Al-4V”, *Rapid Prototyping Journal*, Vol. 23 No. 6, pp. 1051-1056, doi: [10.1108/RPJ-08-2015-0105](https://doi.org/10.1108/RPJ-08-2015-0105).
- Singh, G., Missiaen, J.-M., Bouvard, D. and Chaix, J.-M. (2021), “Additive manufacturing of 17–4 PH steel using metal injection molding feedstock: analysis of 3D extrusion printing, debinding and sintering”, *Additive Manufacturing*, Vol. 47, p. 102287, doi: [10.1016/j.addma.2021.102287](https://doi.org/10.1016/j.addma.2021.102287).
- Sotomayor, M.E., Várez, A. and Levenfeld, B. (2010), “Influence of powder particle size distribution on rheological properties of 316L powder injection moulding feedstocks”, *Powder Technology*, Vol. 200 Nos 1/2, pp. 30-36, doi: [10.1016/j.powtec.2010.02.003](https://doi.org/10.1016/j.powtec.2010.02.003).
- Soyama, H. and Takeo, F. (2020), “Effect of various peening methods on the fatigue properties of titanium alloy Ti6Al4V manufactured by direct metal laser sintering and electron beam melting”, *Materials*, Vol. 13 No. 10, p. 2216, doi: [10.3390/ma13102216](https://doi.org/10.3390/ma13102216).
- Vaithilingam, J., Prina, E., Goodridge, R.D., Hague, R.J.M., Edmondson, S., Rose, F.R.A.J. and Christie, S.D.R. (2016), “Surface chemistry of Ti6Al4V components fabricated using selective laser melting for biomedical applications”, *Materials Science and Engineering: C*, Vol. 67, pp. 294-303, doi: [10.1016/j.msec.2016.05.054](https://doi.org/10.1016/j.msec.2016.05.054).
- Vyas, C., Poologasundarampillai, G., Hoyland, J. and Bartolo, P. (2017), “2 - 3D printing of biocomposites for osteochondral tissue engineering”, in Ambrosio, L. (Ed.), *Biomedical Composites (Second Edition)*, Woodhead Publishing, Sawston, pp. 261-302, doi: [10.1016/B978-0-08-100752-5.00013-5](https://doi.org/10.1016/B978-0-08-100752-5.00013-5).
- Weißmann, V., Drescher, P., Seitz, H., Hansmann, H., Bader, R., Seyfarth, A., Klinder, A. and Jonitz-Heincke, A. (2018), “Effects of build orientation on surface morphology and bone cell activity of additively manufactured Ti6Al4V specimens”, *Materials*, Vol. 11 No. 6, p. 915, doi: [10.3390/ma11060915](https://doi.org/10.3390/ma11060915).
- Wu, A.S., Brown, D.W., Kumar, M., Gallegos, G.F. and King, W.E. (2014), “An experimental investigation into additive manufacturing-induced residual stresses in 316L stainless steel”, *Metallurgical and Materials Transactions A*, Vol. 45 No. 13, pp. 6260-6270, doi: [10.1007/s11661-014-2549-x](https://doi.org/10.1007/s11661-014-2549-x).
- Young, D., Wetmore, N. and Czabaj, M. (2018), “Interlayer fracture toughness of additively manufactured unreinforced and carbon-fiber-reinforced acrylonitrile butadiene styrene”, *Additive Manufacturing*, Vol. 22, pp. 508-515, doi: [10.1016/j.addma.2018.02.023](https://doi.org/10.1016/j.addma.2018.02.023).
- Young, D.J., Otten, C. and Czabaj, M.W. (2019), “Effect of processing parameters on interlayer fracture toughness of fused filament fabrication thermoplastic materials”, in Kramer, S., Jordan, J.L., Jin, H., Carroll, J. and Beese, A.M. (Eds), *Mechanics of Additive and Advanced Manufacturing, Volume 8: Conference Proceedings of the Society for Experimental Mechanics Series*, Springer International Publishing, Cham, pp. 77-79, doi: [10.1007/978-3-319-95083-9_14](https://doi.org/10.1007/978-3-319-95083-9_14).

Corresponding author

Berenika Hausnerova can be contacted at: hausnerova@utb.cz

For instructions on how to order reprints of this article, please visit our website:

www.emeraldgroupublishing.com/licensing/reprints.htm

Or contact us for further details: permissions@emeraldinsight.com